EGFR and HER2 Activate Rigidity Sensing Only on Rigid Matrices

Mayur Saxena[1,*], **Shuaimin Liu**[2,*], **Bo Yang**[3], **Cynthia Hajal**[2], **Rishita Changede**[3], **Junqiang Hu**[2], **Haguy Wolfenson**[4,5], **James Hone**[2], and **Michael P. Sheetz**[3,4]

[1]Department of Biomedical Engineering, Columbia University, New York, New York 10027, USA

[2]Department of Mechanical Engineering, Columbia University, New York, New York 10027, USA

[3]Mechanobiology Institute, National University of Singapore, Singapore 117411, Singapore

[4]Department of Biological Sciences, Columbia University, New York, New York 10027, USA

[5]Department of Genetics and Developmental Biology, The Ruth and Bruce Rappaport Faculty of Medicine, The Technion – Israel Institute of Technology, Haifa, Israel 31096

Abstract

Epidermal growth factor receptor (EGFR) interacts with integrins during cell spreading and motility, but little is known about the role of EGFR in these mechanosensing processes. Here we show, using two different cell lines, that in serum- and EGF-free conditions, EGFR or HER2 activity increase spreading and rigidity-sensing contractions on rigid, but not soft, substrates. Contractions peak after 15–20 min, but diminish by 10-fold after 4 hours. Addition of EGF at that point increases spreading and contractions, but this can be blocked by myosin-II inhibition. We further show that EGFR and HER2 are activated through phosphorylation by Src family kinases (SFK). On soft surfaces, neither EGFR inhibition nor EGF stimulation have any effect on cell motility. Thus, EGFR or HER2 can catalyse rigidity sensing after associating with nascent adhesions under rigidity-dependent tension downstream of SFK activity. This has broad implications for the roles of EGFR and HER2 in absence of EGF both for normal and cancerous growth.

Introduction

The rigidity of the extracellular matrix (ECM) plays a significant role in cell proliferation, differentiation, and motility[1–3]. During spreading and migration, cells mechanically test

ECM rigidity by contracting the matrix to a constant displacement[4]. If the force exceeds a threshold of about 25 pN during the displacement, early integrin adhesions are reinforced[5,6]. Recent studies show that these forces are generated through actomyosin-based sarcomere-like contractile units (CUs) producing nanometer-scale local displacements[6,7]. In addition, tropomyosin 2.1 (Tpm2.1), an important component of the local sarcomeric units, is a tumor suppressor required for anoikis on soft surfaces, reinforcing the idea that the early rigidity sensing process is critical for growth control[6]. AXL and ROR2 are tyrosine kinases that control sarcomeric unit displacement and duration, where AXL phosphorylates Tpm2.1 to catalyze adhesion assembly[8]. All this strongly supports the hypothesis that rigidity sensing is performed by the local sarcomeric contractions. Thus, analysis of the local CUs enables quantitative measurements of the level of rigidity sensing activity over extended time periods.

It is known that growth factor receptors interact with integrins during cell spreading and migration[9–11]. Previous studies have shown that upon acute EGF stimulation, EGFR activates spreading and myosin II contraction, leading to focal adhesion (FA) redistribution[12,13]. In the absence of EGF, EGFR also regulates cellular functions like proliferation and cell cycle control by activation in an adhesion-dependent, ligand-independent manner. Interplay between EGFR and its other isoforms like HER2 has previously been shown to play an important role in several cancers[14] where cellular rigidity sensing is altered. Further, there is a strong link between EGFR and contractility through phospholipase C (PLC) and the activation of protein kinase C (PKC)[15]. At an upstream level, active SFKs are recruited to early integrin adhesions, and in biochemical assays SFKs phosphorylate and activate EGFR[9]. Together, EGFR and the cells' underlying substrate appear to be involved in cellular motility and traction forces. Because rigidity sensing is a fundamental activity during cell spreading and migration, we conjecture that EGFR activation may affect rigidity sensing and early adhesion site formation (focal complexes that are localized at the cell periphery[16,17]).

We analyzed the level of rigidity sensing events in spreading cells as a function of ligand-independent EGFR activity. Surprisingly, EGFR activity was necessary for rigidity sensing on stiff but not on soft surfaces. Further, we found that EGFR activation of rigidity sensing depended upon myosin contractile activity. Thus, EGFR is involved in a positive feedback control of adhesion formation on rigid fibronectin surfaces but is much less active on soft surfaces. These results are consistent with the hypothesis that stretching of an early component in adhesion complexes recruits EGFR that then catalyzes rigidity sensing. Interestingly, we found that the lack of rigidity sensing in the absence/inhibition of EGFR on stiff substrates could be rescued by overexpression of HER2 — the latter having previously been correlated to a variety of cancers[18] — in a Src kinase dependent manner.

Results

Density of local contractile units peaks at early spreading

Previous studies showed that fibroblasts apply local contraction forces to substrates to test their rigidity through local actomyosin-based contractile units (CUs)[5,6]. To detect CUs, cells were here plated on 0.5 μm diameter polydimethylsiloxane (PDMS) pillars coated with

fibronectin (FN) and displacements were tracked in real-time (Fig. 1a). Each rigidity-sensing event was dynamic and transient. One cycle of pulling and release typically lasted 20–40 seconds (Fig. 1b) and was located 1–3 μm from an extending cell edge (Fig. 1a). The previous studies of these CUs focused on early spreading (~30 min)[5,6] but not longer durations. To extend the time range of the measurements, we developed an automated program to measure pillar deflection and identify CUs (see Methods). CUs formed at a relatively constant density in lamellipodial extensions of the cell edge (active areas) but not in stationary regions (static areas; Supplementary Fig. 1a,b). After the initial burst of contractile activity in spreading, the number of CUs dropped dramatically. Thus, there was a strong correlation between the level of spreading and CU activity in control cells (Supplementary Fig. 1c).

When cells were plated on a relatively stiff pillar matrix (bending stiffness = 6 nN/μm, effective modulus = 17.2 kPa, see Methods for calculations), the number of contractile units per cell peaked at ~20 minutes after binding (Fig. 1c). CU activity decreased by about ten-fold in 5 hours and remained low. The peak of CU density in early spreading coincided with the contractile spreading phase P2[19], in which cells tested substrate rigidity by local CUs across their edges[5,6]. After 30–60 minutes of spreading, cell edges were relatively stable; however, small areas moved outward periodically about every 5 minutes on average and those occasioned 5 or more CUs. Thus, the density of CUs was greatest in early spreading, although the cell continued to test the surface rigidity intermittently.

Next, we followed CU activity on soft pillars (effective stiffness=2.5 nN/μm, effective modulus=7.2 kPa) over long time periods (Fig. 1d). On these pillars, cells exhibited a lower level of rigidity sensing activity, evidenced by overall lower CU density (Fig. 1e). Again, occasional extensions activated CUs but those were typically followed by edge retractions giving cycles of extension and retraction over 20–40 minutes. These data were consistent with previous findings that adhesion complexes dissociate due to insufficient force for reinforcement on soft substrates[6].

Ligand-free EGFR activity is necessary for rigidity sensing

Since integrins cooperate with EGFRs in regulating cellular interactions with the extracellular environment[20] and co-cluster with FAK[21], we tested the role of EGFR kinase activity in CU activity during spreading. Previous evidence of integrin-EGFR complexes residing in immature FAs rather than mature FAs[22], indicated that ligand-independent EGFR activation could play an important role in regulating rigidity sensing during early adhesion formation. When cells were plated on FN-coated pillar substrates, in medium lacking serum (growth factors) but containing an EGFR inhibitor, they spread abnormally. Initially, on stiff pillars, the EGFR inhibitor caused slower spreading and cells reached normal P1 areas (the rapid spreading phase without contractions) typically only after ~20 minutes (compared to normal periods of ~3–10 minutes). However, they failed to spread further (Fig. 2a), exhibited a much smaller active area (Supplementary Fig. 2a), and had very few CUs (Fig. 2b). These cells often adopted a dendritic morphology and had narrow extensions instead of broad lamellipodia (Supplementary Fig. 2b). On soft pillars, the EGFR inhibitor was ineffective. Cells spread to a similar overall area and had a similar average CU density with or without

inhibitor (Fig 2c,d). We verified that cells on continuous FN-coated gels of rigidity 5.5 kPa and 50 kPa showed the same rigidity dependence of EGFR inhibition as cells on the pillars (Supplementary Fig. 2c). Thus, the spreading and contractile activity of cells dramatically decreased after EGFR inhibition on rigid but not on soft surfaces.

To confirm that EGFR was the specific isoform involved and not other ErbB isoforms (ErbB2/3/4), we analyzed cos-7 cells, which primarily express ErbB1/EGFR (to enable cos-7s to form rigidity-sensing CUs, they were transfected with myosin-IIA, which is needed for mechanosensing[23] but is not expressed in cos-7s). As expected, the EGFR inhibitor significantly reduced CU formation and spreading area of cos-7s on rigid pillars (Supplementary Fig. 3a,b). Further, upon knockdown of EGFR in cos-7s or mouse embryonic fibroblasts (MEFs), spread area was significantly reduced and EGFR inhibition had no further effect (Supplementary Fig. 3c,d) (notably, many cells died within 6 hours of spreading after EGFR knockdown). It appeared that EGFR activity was needed for contractile-dependent cell spreading and CU formation on stiff surfaces.

Both MEFs and cos-7 cells express low levels of ErbB2 (HER2) and endogenous HER2 does not seem to support contractile activity. However, HER2 is a ligand-independent receptor from the EGFR family sharing several downstream targets with EGFR[14,24]. When HER2 was overexpressed in cos-7 cells (expressing myosin-IIA), EGFR inhibition had no effect on CU activity and spreading area (Fig. 2e,f). However, addition of a small molecule inhibitor for both EGFR and HER2 caused a significant drop in CUs and spreading area, similar to EGFR inhibition of wild-type (WT) cells (Fig. 2a,b). To confirm this rescue, we knocked-down EGFR expression in cos-7s (expressing myosin-IIA) and then overexpressed HER2. Again, these cells had fully restored contractile activity and normal cellular spreading (Fig. 2e,f). Thus, under normal conditions EGFR is involved in the mechanosensing process and there is not enough HER2 to contribute, but HER2 overexpression can replace EGFR function.

Src mediated ligand-independent activation of EGFR

In the absence of ligand, EGFR or HER2 could be activated by Src[25]. To test this in our system, we performed cross-correlation analyses on super-resolution structured illumination microscopy (SIM) images of active phospho-EGFR with paxillin in adhesion sites after immunostaining with an antibody that reacts with a Src-dependent phosphorylation site on EGFR (Y1068). Besides the two aforementioned pillar arrays, we performed these experiments on two substrate extremes: glass coated with RGD ligands (stiff), and lipid bilayers in which RGD ligands diffuse freely (without force) (Fig. 3a–e). We found that paxillin adhesions were not associated with pEGFR on lipid bilayers (Fig. 3a), but on glass pEGFR colocalized with paxillin (confirmed by Pearson's correlation coefficients; Fig. 3e). In many cases on RGD-coated glass, pEGFR was found in nascent adhesions before paxillin recruitment and as adhesions matured the pEGFR/paxillin ratio decreased (Fig. 3f,h). As a control, we stained WT cells with an antibody that reacts with the Src-independent EGFR autophosphorylation site (Y1173) and found a general staining of the cell surface, with no specific localization to active cell edges (Supplementary Fig. 4a,b). These results were further confirmed by measuring the intensity ratio at the cell edge compared to inner cellular

locations (Supplementary Fig. 4a) of pY1068 EGFR as well as another Src-dependent phosphorylation site on EGFR (Y845) on stiff and soft pillars (Supplementary Fig. 4c,d). Furthermore, inhibition of EGFR kinase activity on stiff pillars blocked paxillin and pEGFR co-localization (Supplementary Fig. 2b). Thus, Src-activated EGFR colocalized with integrin clusters at peripheral adhesions only when they were under force.

SFK activation of EGFR is required for rigidity sensing

Since EGFR inhibition was effective on stiff but not on soft pillars, and EGFR activation through Src was force-dependent, we hypothesized that Src-dependent activation of EGFR was required for rigidity sensing. Inhibiting Src activity with PP2 (at concentrations 100–200 nM that blocked only Src kinases but not EGFR) caused a significant decrease in the level of local CU activity, active edges, and spread areas in MEFs (Fig. 4a–c, Supplementary Fig. 5a) as well as in cos-7 cells (Supplementary Fig. 3a,b). To confirm the role of Src-dependent phosphorylation of EGFR, we mutated the Src-dependent phosphorylation site, Y845F, or the autophosphorylation site, Y1045F, and expressed these mutations in cos-7 cells after EGFR knock down. When spread on stiff pillars, CUs and cellular area could not be rescued by the EGFR-Y845F mutant whereas the EGFR-Y1045 mutant performed like WT EGFR (Fig 4c,d). Further, both PP2 addition (Supplementary Fig. 3b) and mutation of the Src phosphorylation site of HER2, Y877F, blocked the ability of HER2 to restore spreading and rigidity sensing in cos-7 cells after EGFR knock down or inhibition (Fig. 4c and Supplementary Fig. 3b). Thus, we suggest that both EGFR and HER2 are activated by SFK activity on rigid surfaces.

To determine which Src kinase was involved, we studied SYF cells that lack major SFKs (Src, Yes and Fyn), and found that pEGFR did not co-localize with paxillin at peripheral adhesion sites (Supplementary Fig. 4e, Supplementary Fig. 5b,c). With stable knock-ins of c-Src, c-Yes or Fyn in SYF cells[26], we found that any of the knock-ins restored colocalization of pEGFR with paxillin (Supplementary Fig. 4f, Supplementary Fig. 5b,c).

Thus, these data indicated that SFK-dependent EGFR or HER2 tyrosine kinase activity play a critical role in promoting rigidity sensing and cell spreading on stiff matrices.

EGF stimulates an increase in rigidity sensing on rigid surfaces

EGF is known to promote cell migration and growth through increased force generation and adhesion formation[27]. Evidence has shown that acute EGF stimulation causes phosphorylation of myosin regulatory light chain (MRLC) to promote myosin-II contraction[15], nearly simultaneously with adhesion assembly and paxillin phosphorylation in the adhesions[13]. Together, direct observations of focal adhesion assembly in cell protrusion areas and increased contraction force induced by acute EGF stimulation[13] led us to hypothesize that EGF also had an effect on local contractile forces that sense rigidity.

To test if EGF stimulated rigidity sensing, we added 100 ng/ml EGF after 6 hours of cell adhesion to FN-coated stiff pillar substrates (17.2 kPa). A large portion of the cell edge moved out ~2 minutes after EGF addition, increasing the cell area (Fig. 5a). After ~15 minutes, the lamellipodia retracted in a large fraction of cells (Supplementary Fig. 6a), rapidly recovering pre-EGF area levels (Fig. 5c). Further, EGF addition caused a dramatic

increase in CU number in extending regions (Fig. 5b). At ~2 minutes after EGF addition, CU density increased dramatically to the levels seen at 15–20 min of spreading (Fig. 5d), and remained at this level for about 10–20 minutes before returning to the basal level after an additional 30 minutes. During the peak of EGF stimulation, local contractile force reached ~30% of total cell contraction force in the extending areas (Supplementary Fig. 6b). These activation events were blocked by the EGFR inhibitor (Fig. 5d, Supplementary Fig. 6c). Thus, on rigid surfaces, EGF activates cell spreading and CU formation through kinase activation.

EGF activation of motility requires myosin contractility and SFK

Next, we tested if myosin-II activity was required for EGF activation. Myosin-II contractile activity was mediated by MRLC[28], which can be phosphorylated by rho-kinase[29] (ROCK). Adding Y-27632 (an inhibitor of myosin-II ROCK-mediated activity) blocked EGF-induced local contractility. Although Y-27632 addition caused a small increase in spread area (Fig. 5e,f), there was no increase in the number of CUs. Further, after treatment with Y-27632 for 20 minutes, EGF stimulation of motility and contractility was lost (Fig. 5f). Thus, inhibition of ROCK-dependent initiation of myosin-II contractility blocked EGF stimulated local contractile activity and cell edge spreading.

To test for a role of SFKs in EGF stimulation, we stimulated MEFs in the presence of PP2 and found that there was no significant area or contractile unit increase post EGF addition (Fig. 5g). Similar results were observed with EGF stimulation of SYF cells (Fig. 5g). Thus, EGF activation of spreading and contractility is downstream of SFK activity.

On soft surfaces EGF has no effect on rigidity sensing or motility

Since EGFR activity was not important for spreading and myosin contractility on soft surfaces, we wondered if EGF addition activated rigidity sensing on soft surfaces. After 6 hours on soft surfaces, cells changed spread area and morphology almost cyclically over periods of 30–45 minutes. When EGF was added to cells on soft pillar substrates, there was no stimulation of spreading or CU activity. The cell area oscillations appeared unaltered following EGF addition (Fig. 5a). Further, EGF stimulation did not alter paxillin immunostaining on these substrates. Although EGF addition caused a significant increase in pEGFR in cells on soft surfaces, most pEGFR was not associated with adhesion complexes, contrary to cells on stiff pillars (Supplementary Fig. 4g and Supplementary Fig. 6d). These data are in line with previous results showing that reducing substrate rigidity desensitizes cells to EGF[30].

Discussion

Our results show that the EGFR and HER2 tyrosine kinases have a previously overlooked yet critical role in rigidity sensing. We find that rigidity sensing is dependent on EGFR activity. Surprisingly, EGFR has a significantly reduced role on soft surfaces, with much less CU activity. This is partly explained by the fact that pEGFR localizes to integrin adhesions considerably more on rigid than on soft substrates. However, EGFR is only transiently associated with adhesions during their development, and once they are mature, their

association with pEGFR is weak (these results are further discussed in Supplementary Discussion).

Furthermore, we show that the recruitment of pEGFR to adhesion sites depends upon SFK. Using mutants of Src-dependent phosphorylation sites we find that this pathway has a major role in the ligand-independent cellular rigidity sensing mechanism. We know that SFKs are activated in very early integrin adhesions and mere binding of soluble ligand to integrins leads to activation of SFKs even in the absence of force[24]. Further, Src phosphorylation is not affected in the absence of talin, a force-bearing component of adhesions. Therefore, it is admissible that rigidity sensing will occur after SFKs are recruited and activated. We postulate that force is unfolding a protein such as talin in the adhesion clusters, which then binds EGFR and holds it for phosphorylation. Active EGFR could then further activate local myosin contraction through the known pathways downstream of EGFR involving PLC-dependent activation of PKC[15]. This positive feedback system could then cause further spreading and further SFK-dependent EGFR activation. Soft surfaces have short-lived adhesions that generate only weak forces, and thus they possibly would not recruit EGFR. Further, such a positive feedback scheme could explain the effect of EGF on formation of new CUs on rigid but not on soft surfaces or after inhibition of myosin contraction. Thus, we suggest that cell spreading and adhesion development involves EGFR in the formation but not in the maintenance of adhesions. All the evidence indicates that EGFR has a critical role in rigidity sensing that is dependent upon substrate rigidity and mechanical force. Although EGFR may have other roles that do not depend upon rigidity, it is clear both in the absence and presence of EGF that EGFR activity dramatically increases rigidity sensing on rigid surfaces and activates cell growth.

Methods

Procedure for Contractile unit (CU) Quantification

For measurement of CUs, movements of pillars within about 4 micrometers of the cell edge were analysed. To allow for measurement of absolute displacement of the pillars, we followed pillars that were not initially in contact with the cell, but were beneath it after cell spreading. Data files with the position coordinates of cellular pillars and reference pillars were obtained from ImageJ Nano tracking plugin as described in the section 'Tracking pillar movements'. These data were then imported to a Matlab program to automatically generate force vector maps for the detected CUs and output the number of CUs per frame. Threshold parameters were set by users to identify CUs, including the time threshold (e.g. 20 s for MEFs), displacement threshold (>20 nm for 20 s) and space threshold (i.e. distance between neighbouring pillars). Therefore, CUs were identified on freshly contacted pillars with a detection criterion requiring that two or more neighboring pillars were pulled toward each other by more than 20 nm and for more than 20 seconds.

To verify the method, we visually counted the number of CUs then compared those results to the results generated by the program: miscounted CUs arose in cases when a pair of pillars that pointed perpendicular to each other were recognized as CUs (Supplementary Fig. 1a). The overall success rate of the automatic detection algorithm was 97.47±0.75% compared to the manual analysis.

Tracking pillar movements

Time-lapse imaging of pillars was performed with bright-field microscopy using an ORCA-Flash2.8 CMOS camera (Hamamatsu) attached to an inverted microscope (Olympus IX-81), controlled by Micromanager software[31]. Images were recorded at 1 Hz using a 60× 1.4 NA, oil immersion objective (yielding a pixel size of 36 nm/pixel).

Videos were processed with ImageJ (National Institutes of Health) using the Nano Tracking plugin to track the position of pillars as explained previously[5,6]. The Nano Tracking plugin was based on a robust cross-correlation algorithm (resistant to particle shape variation) to track the position of pillars, and programmed to enable users to track all pillars in the appropriate areas automatically. To account for stage drift and illumination fluctuation, we analysed the movements of a set of reference pillars outside the cell, and subtracted their averaged movements from the movements of the pillars of interest. A low-pass filter (5 frame median filter) was used to smooth the stabilized movie before analysis for CUs.

Long-term CU measurement experiments

To reduce photo-damage to the cells during the long-term imaging, we tracked pillar movements intermittently for periods of 5–10 minutes every 30 or 60 minutes. When cells were observed with this protocol, there was no discernable photo-damage and this was validated by observing cells in the same dish at later times that had not previously been monitored. Thus, the method enabled us to monitor the number of CUs per cell for extended time periods. Cells were kept in a 37°C, 5% CO_2 chamber on an inverted microscope, and a >600nm filter was used to reduce photodamage during imaging.

Continuous imaging over extended periods, i.e., imaging at 1 Hz for many hours, led in many cases to a halt in cell spreading and later to blebbing and apoptosis. With the typical protocol that we used (tracking of the pillar movements for periods of 5–10 minutes every half hour) we did not detect these effects. Further, cells that were imaged in this way for >6 hours appeared very similar to other cells in the dish that were not illuminated during this period.

Pillar fabrication

Molds for making PDMS pillars were fabricated using electron beam lithography in hard Poly(methyl methacrylate) (PMMA) substrates. PMMA was first spun-coated onto a silicon substrate and then hard-baked on a hot plate for 10 hours. An electron beam lithography tool (NanoBeam nB5) was then used to pattern holes in the PMMA. The depth of holes was determined by the thickness of the PMMA. PDMS (mixed at 10:1 with its curing agent, Sylgard 184; Dow Corning) was then poured onto the PMMA moulds, cured at 70 °C for 12 h to reach a Young modulus of 2 ± 0.1 MPa, and demolded while immersed in 99.5 % isopropanol. All pillars had diameter D = 500 nm with a 1000nm pitch. The top surfaces of the pillars were flat, with a height variation of only ~10% of pillar diameter. Pillar bending stiffness, k, was calculated by Euler–Bernoulli beam theory:

$$k = \frac{3}{64}\pi E \frac{D^4}{L^3}$$

where D and L are the diameter and length of the pillar, respectively, and E is the Young's modulus of the material (PDMS). k was further multiplied by a correction factor to take into account substrate warping at the base of the pillars[32]. In this paper, two different heights of pillars were fabricated for a stiff surface with effective modulus of 17.2 kPa (L1300 nm, effective stiffness=6 nN/μm) and a soft surface with effective modulus of 7.2 kPa (L1800, effective stiffness=2.5 nN/μm). The effective stiffness was calculated in accordance to the equation:

$$E\,(effective) = \frac{9}{4}\frac{k}{\pi A}$$

Where A is the typical length of adhesions forming on pillars[33].

The surfaces of the PDMS pillar substrates were coated with 10 μg/ml fibronectin for at least 1 hour prior to seeding cells. Scanning electron microscopy of fixed samples revealed that cell membranes only contacted the upper surface of the pillars and did not extend between pillars.

Flat substrate fabrication and preparation

For the 5.5 kPa substrate PDMS (1:1 Sylgard 527 part A:part B::1:1) was spread on glass bottom dishes and then incubated at 70°C for 12 h. To achieve 50 kPa we mixed the Sylgard 527 mixture with Sylgard 184 mixture in accordance to the previously developed methods[34] and then incubated at 70°C for 12 h. The surfaces of the PDMS gels were coated with 10 μg/ml fibronectin for at least 1 hour prior to seeding cells. Rigidity of the PDMS surfaces was measured by atomic force microscopy (AFM) indentation.

Cell Culture and Reagents

Mouse embryonic fibroblasts (MEFs) cells were generated by J. Sap's laboratory[35]. The cells were cultured at 37° C in a 5% CO_2 incubator in Dulbecco's Modified Eagle Medium (DMEM) supplemented with 10% fetal bovine serum (FBS), 100 IU/ml Penicillin-Streptomycin, and 2 μM L-Glutamine. The cells were tested for mycoplasma contamination and found negative. In all experiments, cells were serum-starved in growth medium lacking FBS. Imaging experiments were conducted using starvation medium without phenol red. Growth factors (all from Life Technologies) were diluted into 0.5 ml medium before adding to the specimen. The specific hormones used were mouse recombinant EGF (100 ng/ml) and mouse recombinant TGFβ$_1$ (10 ng/ml). Pharmacological inhibitors and antibodies were as follows: Y-27632 (20μM, Calbiochem, Gibbstown, NJ), gefitinib (10 nM, Santa Cruz), PP2 (200 nM, abcam), pEGFR Tyr1173 (Santa Cruz, sc-12351), pEGFR Y1092 (abcam, equivalent to Y1068, EP774Y), paxillin (abcam, ab3127, 5H11, ab32084, BD Biosciences, 612405), pEGFR Y845 (abcam, ab5636), EGFR1 (abcam, ab30).

Several shRNA for EGFR were bought from Sigma Aldrich and tested. The knockdown results shown are with the shRNA TRCN0000055220 having the sequence "CCGGCCAAGCCAAATGGCATATTTACTCGAGTAAATATGCCATTTGGCTTGGTTTTTG". MEFs were transfected with Lipofectamine LTX using 4μg plasmid on Day 0 and then selected for transfection using Puromycin till all control cells died (Day 4 in our case). Then the selected transfected cells were used in the spreading experiment protocol.

Myosin IIA transfected Cos7 cells (Cos7-IIA) were selected using fluorescence activated cell sorting (FACs) and cultured in Dulbecco's modified Eagle's medium (DMEM) high glucose supplemented with 10% FBS, 1 mM sodium pyruvate (Invitrogen) and 250 μg/ml selective antibiotics (G418) at 5% CO_2 at 37°C.

EGFR-GFP (plasmid #32751), EGFR-Y1045F-GFP (plasmid #40267), HER2-YFP (plasmid #66948) plasmids were purchased from Addgene. The EGFR-Y845F and HER2-Y879F (Rat sequence, equal to Human sequence Y877) mutants were generated using primers 5′AGAGAAAGAATTCCATGCAGAAGGAGG3′ (EGFR), 5′TCCGCACCCAGCAGTTG-3′ (EGFR), 5′TGAGACAGAGTTCCATGCAGATG-3′ (HER2), 5′-TCAATGTCCAGCAGCCGA3′ (HER2), following the protocol provided in Q5 Site-Directed Mutagenesis Kit (NEB). Cells were seeded into a 6-well plate with 60–70% confluence at day 0 and transfected with 25 μM of EGFR siRNA (Qiagen, pre-mix EGFR siRNA, catalogue no. SI00300104) using lipofectamine RNAiMAX (Invitrogen) on day 1. Control cells were transfected with scrambled control siRNA. Transfection of rescue plasmids were performed on day 3 using lipofactamine 2000 (Invitrogen) following the manufacturer's instructions.

Quantification of peripheral localization of pEGFR

In order to assess the population of cells showing peripheral localization of pEGFR we used a relative intensity ratio metric calculated on images of cells stained for various pEGFR sites when spread on different rigidities. Cells were stained and then imaged using the exact same imaging conditions. Two areas - peripheral area (Area 1, up to 5 micrometers from the edge) near the cell edge and inner area (Area 2) - were marked on the image (Supplementary Fig. 3a). Then the Intensity ratio (I) was calculated as:

$$Intensity\ Ratio\ (I) = \frac{Mean\ Intensity\ Area\ 1}{Mean\ Intensity\ Area\ 2}$$

This ratio was a measure of relative localization of intensity near the cell edge.

Statistical Analyses

Sample sizes were chosen to test whether the distributions of the populations were normal, and t-tests were performed where noted. In the case of pEGFR colocalization with paxillin, analyses were performed by calculating the Pearson's correlation coefficient between the two channels.

For long-term live cell tracking, the number of samples was ~10 in each case; however, we compared the results from the live cell movies to randomly chosen cells on the dish at specific time points (the latter n was >30), and the results were comparable.

Code Availability

MATLAB code used for identifying CUs is available upon request.

Data Availability Statement

The data that support the findings of this study are available from the corresponding author upon reasonable request.

Supplementary Material

Refer to Web version on PubMed Central for supplementary material.

Acknowledgments

References

1. Wang HB, Dembo M, Wang YL. Substrate flexibility regulates growth and apoptosis of normal but not transformed cells. Am J Physiol Cell Physiol. 2000; 279:C1345–1350. [PubMed: 11029281]

2. Engler AJ, Sen S, Sweeney HL, Discher DE. Matrix elasticity directs stem cell lineage specification. Cell. 2006; 126:677–89. [PubMed: 16923388]

3. Lo CM, Wang HB, Dembo M, Wang YL. Cell movement is guided by the rigidity of the substrate. Biophys J. 2000; 79:144–52. [PubMed: 10866943]

4. Elosegui-Artola A, et al. Rigidity sensing and adaptation through regulation of integrin types. Nat Mater. 2014; 13:631–637. [PubMed: 24793358]

5. Ghassemi S, et al. Cells test substrate rigidity by local contractions on submicrometer pillars. Proc Natl Acad Sci U A. 2012; 109:5328–33.

6. Wolfenson H, et al. Tropomyosin controls sarcomere-like contractions for rigidity sensing and suppressing growth on soft matrices. Nat Cell Biol. 2016; 18:33–42. [PubMed: 26619148]

7. Meacci G, et al. α-Actinin links extracellular matrix rigidity-sensing contractile units with periodic cell-edge retractions. Mol Biol Cell. 2016; 27:3471–3479. [PubMed: 27122603]

8. Yang B, et al. Mechanosensing Controlled Directly by Tyrosine Kinases. Nano Lett. 2016; 16:5951–5961. [PubMed: 27559755]

9. Sato KI. Cellular functions regulated by phosphorylation of EGFR on Tyr845. Int J Mol Sci. 2013; 14:10761–10790. [PubMed: 23702846]

10. Bill HM, et al. Epidermal growth factor receptor-dependent regulation of integrin-mediated signaling and cell cycle entry in epithelial cells. Mol Cell Biol. 2004; 24:8586–8599. [PubMed: 15367678]

11. Huveneers S, Danen EHJ. Adhesion signaling – crosstalk between integrins, Src and Rho. J Cell Sci. 2009; 122:1059–1069. [PubMed: 19339545]

12. Eberwein P, et al. Modulation of focal adhesion constituents and their down-stream events by EGF: On the cross-talk of integrins and growth factor receptors. Biochim Biophys Acta BBA - Mol Cell Res. 2015; 1853:2183–2198.

13. Schneider IC, Hays CK, Waterman CM. Epidermal Growth Factor–induced Contraction Regulates Paxillin Phosphorylation to Temporally Separate Traction Generation from De-adhesion. Mol Biol Cell. 2009; 20:3155–3167. [PubMed: 19403690]

14. Moasser MM. The oncogene HER2: its signaling and transforming functions and its role in human cancer pathogenesis. Oncogene. 2007; 26:6469–6487. [PubMed: 17471238]

15. Iwabu A, Smith K, Allen FD, Lauffenburger DA, Wells A. Epidermal growth factor induces fibroblast contractility and motility via a protein kinase C delta-dependent pathway. J Biol Chem. 2004; 279:14551–14560. [PubMed: 14747473]

16. Geiger B, Bershadsky A, Pankov R, Yamada KM. Transmembrane crosstalk between the extracellular matrix and the cytoskeleton. Nat Rev Mol Cell Biol. 2001; 2:793–805. [PubMed: 11715046]

17. Wolfenson H, Lavelin I, Geiger B. Dynamic regulation of the structure and functions of integrin adhesions. Dev Cell. 2013; 24:447–58. [PubMed: 23484852]

18. Ménard S, Tagliabue E, Campiglio M, Pupa SM. Role of HER2 gene overexpression in breast carcinoma. J Cell Physiol. 2000; 182:150–162. [PubMed: 10623878]

19. Giannone G, et al. Periodic lamellipodial contractions correlate with rearward actin waves. Cell. 2004; 116:431–43. [PubMed: 15016377]

20. Cabodi S, et al. Integrin regulation of epidermal growth factor (EGF) receptor and of EGF-dependent responses. Biochem Soc Trans. 2004; 32:438–442. [PubMed: 15157155]

21. Yamada KM, Even-Ram S. Integrin regulation of growth factor receptors. Nat Cell Biol. 2002; 4:E75–E76. [PubMed: 11944037]

22. Balanis N, Carlin CR. Mutual cross-talk between fibronectin integrins and the EGF receptor: Molecular basis and biological significance. Cell Logist. 2012; 2:46–51. [PubMed: 22645710]

23. Cai Y, et al. Nonmuscle myosin IIA-dependent force inhibits cell spreading and drives F-actin flow. Biophys J. 2006; 91:3907–20. [PubMed: 16920834]

24. Seshacharyulu P, et al. Targeting the EGFR signaling pathway in cancer therapy. Expert Opin Ther Targets. 2012; 16:15–31. [PubMed: 22239438]

25. Xu KP, Yin J, Yu FSX. SRC-family tyrosine kinases in wound- and ligand-induced epidermal growth factor receptor activation in human corneal epithelial cells. Invest Ophthalmol Vis Sci. 2006; 47:2832–2839. [PubMed: 16799022]

26. Iskratsch T, et al. FHOD1 Is Needed for Directed Forces and Adhesion Maturation during Cell Spreading and Migration. Dev Cell. 2013; 27:545–59. [PubMed: 24331927]

27. Lauffenburger DA, Horwitz AF. Cell migration: a physically integrated molecular process. Cell. 1996; 84:359–69. [PubMed: 8608589]

28. Adelstein RS, Anne Conti M. Phosphorylation of platelet myosin increases actin-activated myosin ATPase activity. Nature. 1975; 256:597–598. [PubMed: 170529]

29. Matsui T, et al. Rho-associated kinase, a novel serine/threonine kinase, as a putative target for small GTP binding protein Rho. EMBO J. 1996; 15:2208–2216. [PubMed: 8641286]

30. Kim JH, Asthagiri AR. Matrix stiffening sensitizes epithelial cells to EGF and enables the loss of contact inhibition of proliferation. J Cell Sci. 2011; 124:1280–1287. [PubMed: 21429934]

31. Stuurman N, Edelstein AD, Amodaj N, Hoover KH, Vale RD. Computer Control of Microscopes using µManager. Curr Protoc Mol Biol Ed. Frederick M Ausubel Al. 2010; CHAPTER(Unit14.20)

32. Schoen I, Hu W, Klotzsch E, Vogel V. Probing Cellular Traction Forces by Micropillar Arrays: Contribution of Substrate Warping to Pillar Deflection. Nano Lett. 2010; 10:1823–1830. [PubMed: 20387859]

33. Ghibaudo M, et al. Traction forces and rigidity sensing regulate cell functions. Soft Matter. 2008; 4:1836–1843.

34. Palchesko RN, Zhang L, Sun Y, Feinberg AW. Development of polydimethylsiloxane substrates with tunable elastic modulus to study cell mechanobiology in muscle and nerve. PLoS One. 2012; 7:e51499. [PubMed: 23240031]

35. Su J, Muranjan M, Sap J. Receptor protein tyrosine phosphatase alpha activates Src-family kinases and controls integrin-mediated responses in fibroblasts. Curr Biol. 1999; 9:505–11. [PubMed: 10339427]
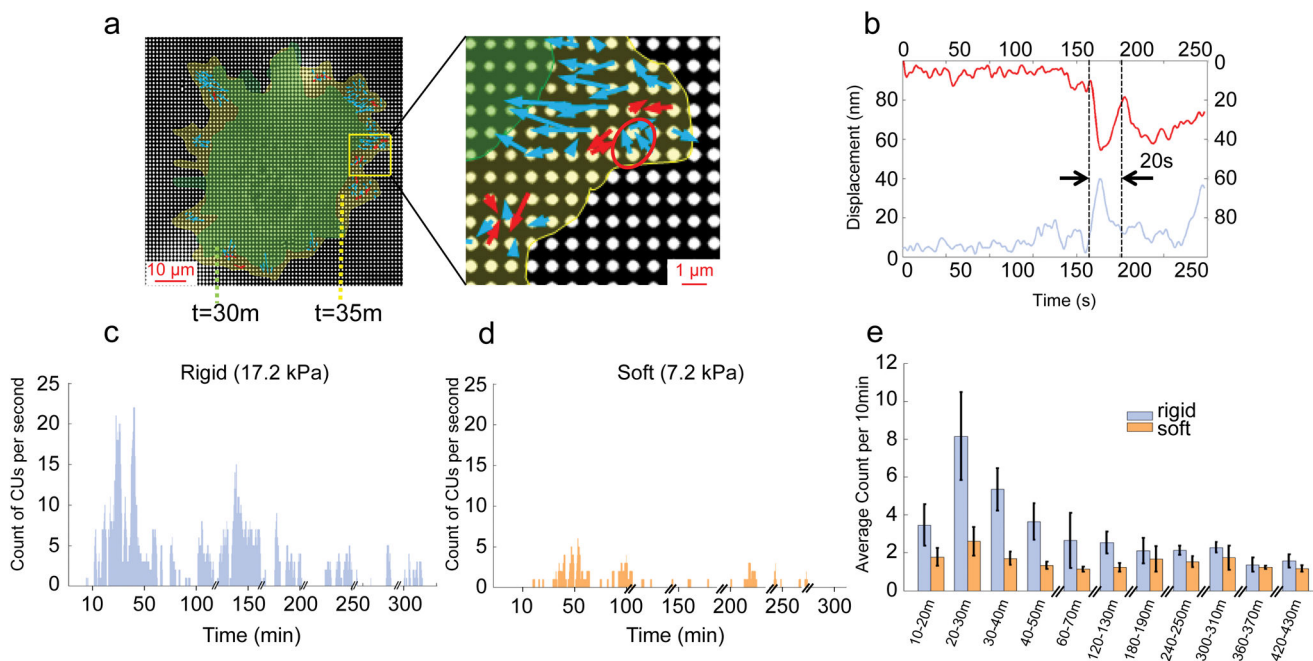
Figure 1.

Rigidity sensing activity measured by local CUs number. **a**, Actual CUs observed at the outward extending edge of a cell spreading on FN-coated 17.2 kPa pillars. Arrows represent pillar movement: red, detected CUs; blue, non-CUs. The red circle marks an example of a correctly identified CU. Cell edges marked in green and yellow correspond to time points 30 and 35 minutes respectively. **b**, Displacement vs. time of two 0.5 μm pillars (red and blue curve) that composed a CU (circled in a). The dotted lines mark the beginning and end time point of the CU. **c,d**, Measurement of CUs per entire cell per second for rigid (**c**) and soft (**d**) pillars. Cells were plated on FN-coated pillar substrate in media lacking serum for over 7 h. **e**, Average number of CUs per 10 min for cells on two pillar substrates of different stiffness in media lacking serum. n>10 cells per condition. n>5 independent experiments. Error bars show standard error of the mean.
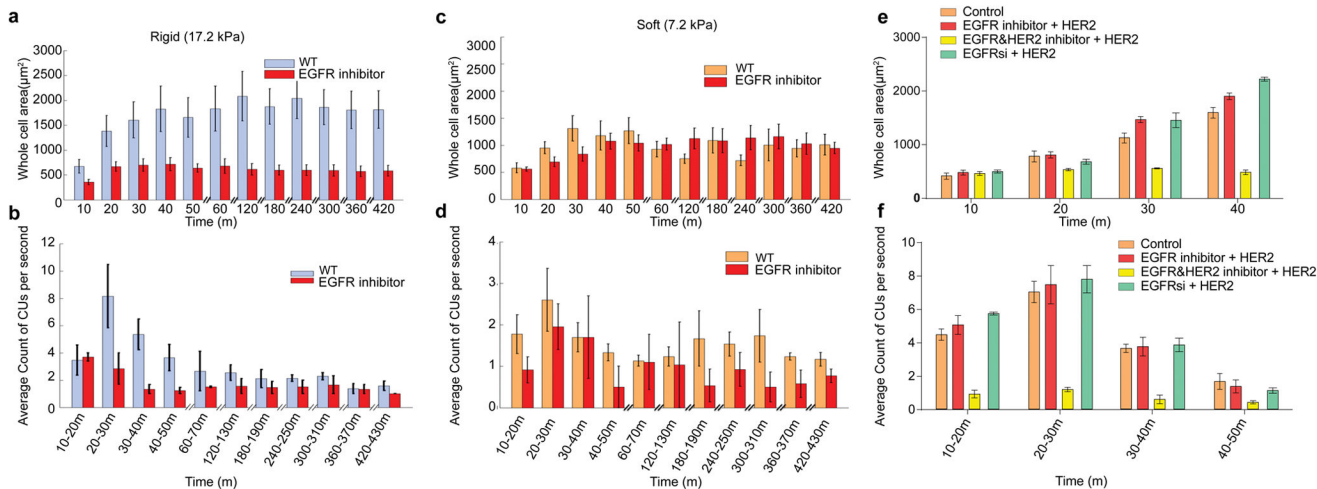
Figure 2.
Ligand-free EGFR and HER2 activity affects local CUs. **a,c**, Increment of cell area
normalized to initial size with respect to time. Cells were plated on FN-coated stiff (**a**) and
soft (**c**) pillar substrates in serum-free medium with and without 10 nM EGFR inhibitor
gefitinib (n ≥ 10 cells for each condition, n>5 independent experiments). **b,d**, Average of
number of CUs per second for 10 min windows monitored for 7 hours on stiff (**b**) and soft
(**d**) substrates. **e**, Areas of cos-7 cells expressing myosin IIA and transfected with the HER2
plasmid. They are spread on stiff pillars in the presence or absence of EGFR inhibitor,
EGFR+HER2 inhibitor, or HER2 siRNA. **f**, Average number of CUs per second in 10
minute windows for the cells in **e**. Error bars show standard error of the mean in all cases.
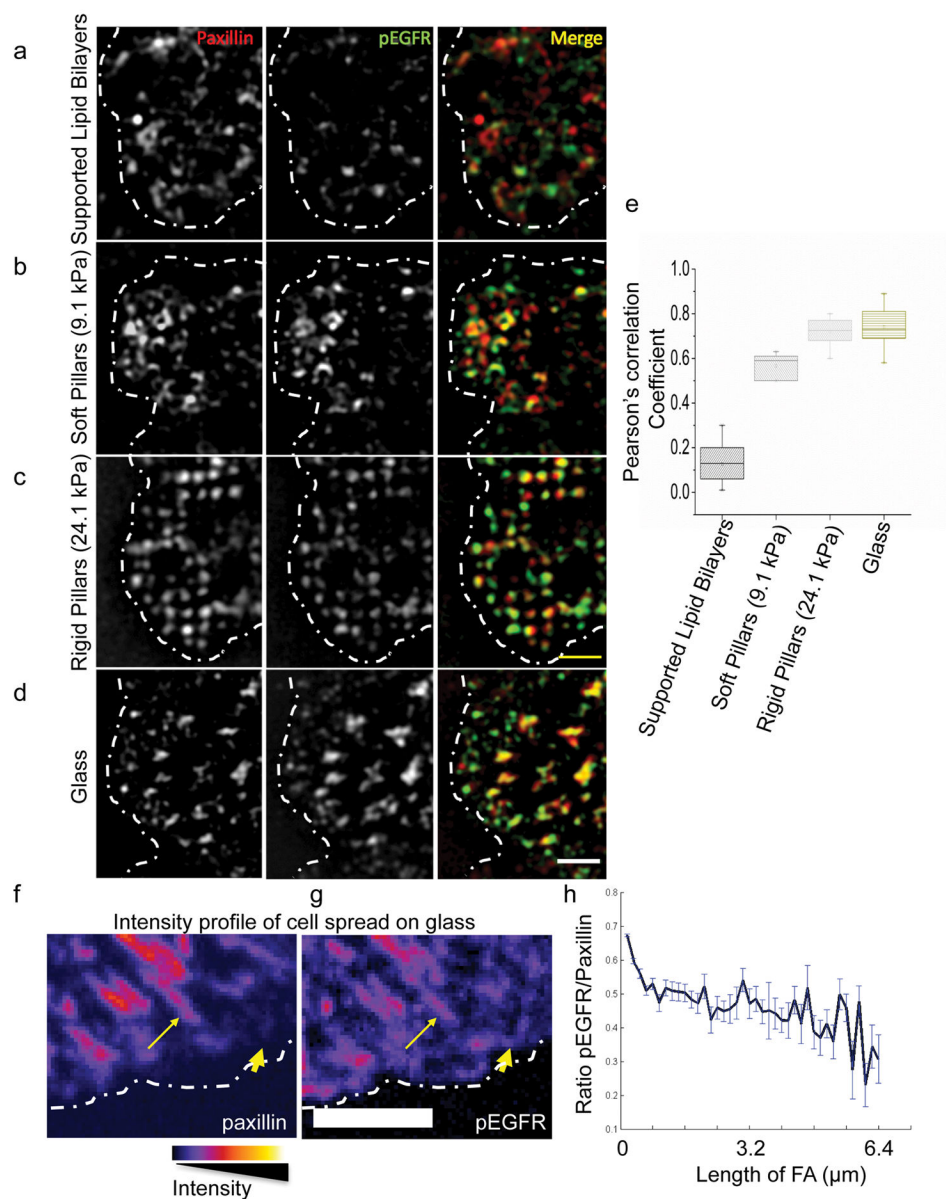
Figure 3.
pEGFR localizes to early adhesions on rigid substrates. **a–d,** A region of MEF-WT spread on supported lipid bilayers (15 minutes), soft (7.2 kPa) or rigid pillars (17.2 kPa; 25 minutes), or on glass (10 minutes), stained for paxillin (red) and pEGFR (Y1068, green), and imaged using structured illumination microscopy. Dotted white line marks the cell boundary. Scale bar is 2μm. **e,** Pearson's correlation coefficient between paxillin and pEGFR measured for cells spread on different substrates. 30>n>10. For cells spread on pillars, colocalization was analyzed on a set of 6–8 pillars near the leading edge of the cell. **f–g,** Pseudo color images taken with confocal microscope (scale shown below) of MEF-WT spread on glass stained for paxillin (**f**) and pEGFR (Y1068; **g**). Dotted line marks the cell boundary. Thick arrows mark localization to early adhesions and thin arrows mark
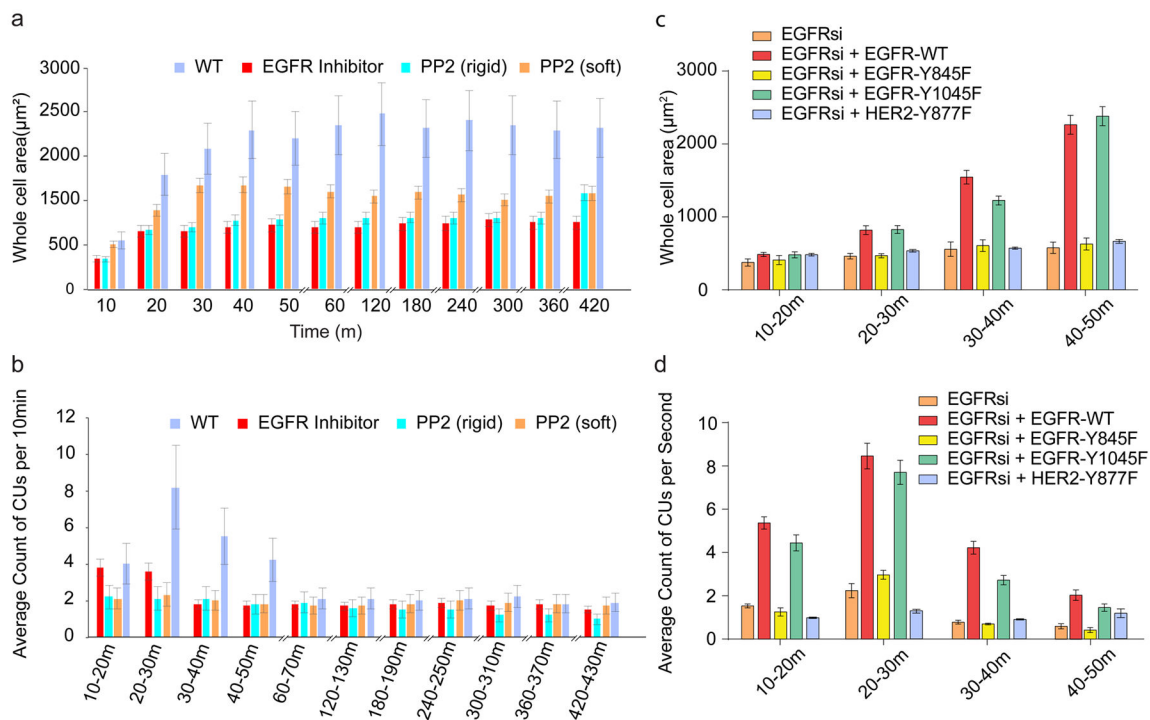
localization to maturing adhesions. Scale bar is 5 μm. **h** Ratio of pEGFR intensity to paxillin intensity in adhesions of increasing size. Error bars show standard error of the mean.
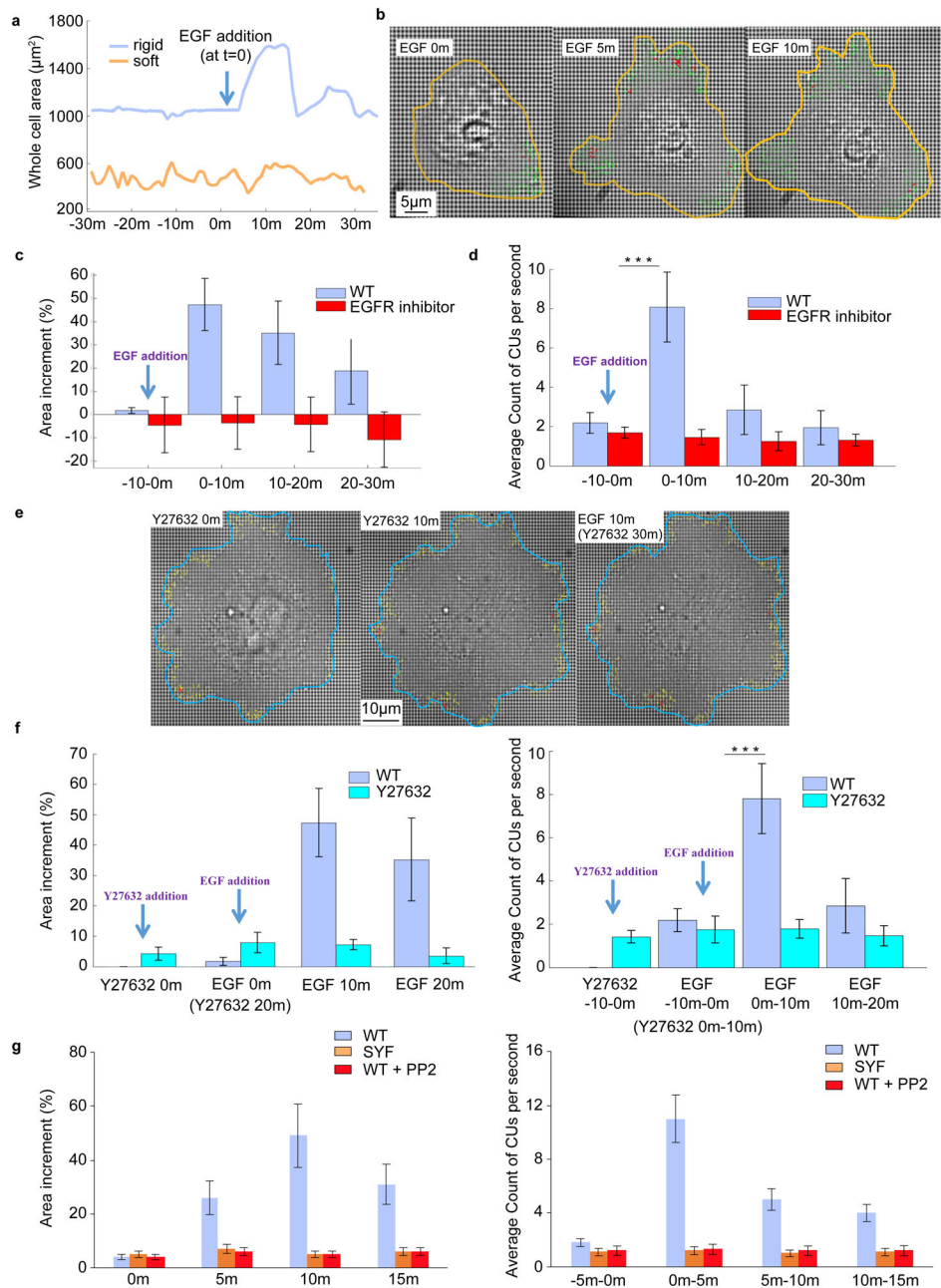
Figure 4.
EGFR and HER2 affect local contractility through Src. **a**, Cell area with respect to time. Cells were pre-incubated with PP2 (200 nM) for 30 min prior to plating on FN-coated pillar substrates in serum-free medium. n>15 cells, n>5 independent experiments. **b,** Average of number of CUs per 10 min monitored for 7 hours. **c**, Area of Cos-7 cells expressing myosin IIA when transfected with siRNA for EGFR and mutations of EGFR or HER2 on FN coated stiff pillars. **d**, Average number of CUs in 10 minute windows for the cells shown in **c.** Error bars show standard error of the mean.

Figure 5.
EGF activates local contraction activity. **a,** EGF (100 ng/ml) addition leads to outward movement of the cell edge on a rigid pillar substrate (blue curve) but not on a soft (orange curve). Cells were plated on FN-coated pillar substrates for 6 h in media lacking serum prior to EGF administration. **b,** Visualization of cell edge extension and increased CU numbers caused by EGF. The yellow line marks the cell edge at each time point after addition of EGF. The green arrows represent the pillar displacement in the active area, while red arrows mark CUs. **c,d,** Area and number of CUs change upon EGF addition. Measurements were carried out in two conditions: with or without EGFR inhibitor pretreatment for 20 min prior to EGF

addition. **c**, Percentage of increased area of the whole cells measured at 0, 10, 20, and 30 min relative to the baseline area (-10 min). **d**, Average over 10 minutes of number of CUs per second before and after addition of EGF for the cells in **c. e**, Visualization of the development of cell area with time upon ROCK inhibition and EGF treatment. After 6 h plating on stiff pillar substrate, cells were treated with 10 μM Y-27632 for 20 min followed by EGF stimulation. Blue line marks the cell edge at each mentioned time point after the addition of EGF. The yellow arrows represent pillar displacement in the active area and red arrows mark CUs. **f**, Y-27632 was added to cells at minute 0. EGF was added to cells at minute 20. *Left:* percentage of increased area measured at 0 min with Y-27632, 20 min with Y-27632, 10 min with EGF, and 20 min with EGF relative to baseline area (10 min before addition of Y-27632). *Right:* average over windows of 10 minutes of number of CUs per second. **g**, Measurements similar to the ones performed in **c** were carried for three conditions: MEFs with or without PP2 inhibitor, and SYF cells. *Left:* percentage of increased area of the whole cells measured at 0, 5, 10, and 15 min relative to baseline area (-5 min). *Right:* average over 5 minutes of number of CUs per second before and after addition of EGF. n>10 for each condition. n>5 independent experiments. Error bars show standard error of the mean. ***p<0.001, student's t-test